Reliability Engineering and System Safety 217 (2022) 108080

Contents lists available at ScienceDirect

Reliability Engineering and System Safety

journal homepage: www.elsevier.com/locate/ress

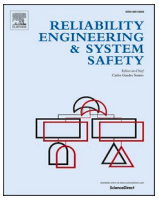

A unified approach for global sensitivity analysis based on active subspace and Kriging

Changcong Zhou [a,*], Zhuangke Shi [a], Sergei Kucherenko [b], Haodong Zhao [a]

[a] Department of Engineering Mechanics, Northwestern Polytechnical University, Xi'an, China
[b] Imperial College London, London SWT 2AZ, UK

ARTICLE INFO

Keywords:
Global sensitivity analysis
Active subspaces
Kriging
Model reduction

ABSTRACT

A global sensitivity analysis (GSA) approach based on the theory of active subspaces and Kriging surrogate metamodeling is developed. Three GSA measures, namely the derivative-based global sensitivity measure (DGSM), activity score and Sobol' total effect indices can be obtained at different steps of the proposed approach. Firstly, by estimating the covariance-like matrix $\boldsymbol{C}$ of response gradients values of DGSM are obtained. Then, the active subspace is identified by using the eigenvalue decomposition of the matrix $\boldsymbol{C}$ and obtained eigenvalues are used to estimate the activity score. In the active subspace, the Kriging model is built by an adaptive process. It is further used for estimation of Sobol' total effect indices. Several test cases are examined to demonstrate the applicability of the proposed approach. They show how it provides different aspects of information from a single set of model runs. The proposed approach is then applied to a radome structure in fiber reinforced composites to find the most significant inputs for its safety.

1. Introduction

Sensitivity analysis studies how the uncertainty in the model output can be apportioned to the uncertainty in model inputs [1]. It can be used for analysis of complex models involving many inputs to identify inputs that have big impacts and those with negligible effect on the model outputs [2]. Such information can be further used for model dimension reduction by fixing unimportant inputs at their nominal values. There are two types of SA: local sensitivity analysis (LSA) and global sensitivity analysis (GSA) [3]. LSA is often formulated as the partial derivative of model outputs with respect to input parameters, and it reflects a change of model output corresponding to a change of parameters in a fixed point in the parameter space. For example, a frequently used LSA index is the reliability-based sensitivity, which is defined in the form of derivatives of failure probability to the parameters [4]. It measures the influence of input parameters to the failure probability, and can be also used by gradient-based algorithms in the reliability-based design optimization. GSA measures the effects of input variables on the model output by considering their whole ranges of definition or distributions [5]. It has been intensively studied in the literature, including GSA index based on reliability [6], variance-based sensitivity index [7], moment-independent importance measures [8], quantile based global sensitivity measures [9]. Among the different GSA measures, the most popular one is the variance-based method of Sobol' sensitivity indices [10,11]. When a new GSA method is introduced, its performance is often compared with the variance-based indices [12]. Another significant GSA measure is the derivative-based global sensitivity measure (DGSM) [13], which is defined as the average of squared partial derivative over the whole input space. The DGSM can be seen as an enhanced and global version of the screening technique proposed by Morris [14]. Sobol' and Kucherenko [15] showed that there is a link between the DGSM and variance-based sensitivity indices in a form of inequality relationship between the DGSM and total effect indices. Lamboni et al. [16] extended definitions of DGSM for different distributions.

Although the GSA theory is a very useful tool for analysis of complex models, its practical usage can be computationally very expensive [17]. Direct computation of GSA indices requires application of the very time-consuming Monte Carlo simulation (MCS) method. To address this issue, many methods have been developed to improve the efficiency of GSA. Among these methods, the surrogate model-based methods became very popular among practitioners. The surrogate model (also known as metamodel) is an approximation of the real model [18], and accuracy of GSA analysis applied to a surrogate model depends on the accuracy of the surrogate model. A review on surrogate model-based

* Corresponding author.
E-mail address: changcongzhou@nwpu.edu.cn (C. Zhou).

https://doi.org/10.1016/j.ress.2021.108080
Received 8 April 2021; Received in revised form 9 September 2021; Accepted 11 September 2021
Available online 20 September 2021

methods including Kriging, support vector machine, radial basis function, polynomial chaos expansion, etc., can be found in Ref. [19]. Among these models, Kriging is the most popular. Not only it provides model predictions, but also it estimates a variance of predictions in the whole domain of inputs [20]. Many surrogate models suffer from the so-called "curse of dimensionality" [21]. Training of a surrogate model also requires more computational efforts when the input dimension is high.

The active subspace theory is developed recently and has become a new valuable method among tools of GSA [22]. As pointed out by Constantine [22], the output of a model may only depend on a limited number of directions in the input space. Each direction corresponds to a linear combination of the original input variables, which is referred to as the active subspace. The active subspace can be identified by performing the eigenvalue decomposition of the covariance-like matrix of response gradients. As the original input variables can be mapped into the active subspace, the input-output model can be set in the active subspaces. For many practical problems there are only a few active directions, thus the model in the subspace becomes a low-dimensional one, which is easier to deal with than with the original model. The active subspace theory has been applied to different areas [23,24]. Constantine and Diaz [25] proposed a new sensitivity index called the activity score, based on the process of finding the active subspace, and showed that the activity score can be interpreted as a truncation of the DGSM.

As the active subspace theory can identify the important directions of the input space, i.e., the active subspaces, thus building the surrogate model in the active subspaces seems to be able to overcome the so-called "curse of dimensionality" mentioned above. It can be appealing for high-dimensional problems. Thus, we propose a method that combines a few efficient ways to realize this idea, and use it to perform GSA. This approach is based on the application of active subspaces followed by Kriging for building a surrogate model in the reduced space. Three types of GSA measures, that is DGSM, activity score and Sobol' total effect indices can be obtained at different steps of the approach. Sobol' total effect indices measures the contribution made by an input variable itself as well as its interactions with the other variables. Firstly, the covariance-like matrix of response gradients is calculated. At this step, the DGSM can be obtained. Then, the eigenvalue decomposition of the gradient matrix is performed to identify the active subspace, and the activity score is estimated on this step. In the active subspace, the mapping between the active variables and the original model output is approximated by an adaptive Kriging process. Once the relationship between the original input variables and the active variables is established, the model output corresponding to any given input sample can be easily obtained with the built Kriging metamodel. Finally, total effect indices are estimated using known MC estimators applied to the Kriging metamodel. Using the proposed approach, a model can be efficiently analyzed, and more information can be provided than with other methods.

The remainder of the paper is organized as follows. The variance-based sensitivity indices and DGSM are briefly reviewed in Section 2. The general principles of active subspaces as well as the activity score index are discussed in Section 3. In Section 4, the detailed procedure of the proposed approach is presented. Several examples are examined in Section 5 to demonstrate the applicability of the proposed approach, and it is also applied to a composite radome to identify the significant inputs for the structural safety. Conclusions are made in Section 6.

2. Review of the variance-based sensitivity analysis and DGSM

2.1. Variance-based sensitivity indices

Consider a square integrable model denoted as $y = f(\boldsymbol{x})$, where y is the output, and $\boldsymbol{x} = [x_1, x_2, ..., x_n]^{\mathrm{T}}$ is the vector of input variables. Based on the technique of ANOVA decomposition also known as high-dimensional model representation (HDMR), the above model can be expanded as follows [10,11]

$$y = f_0 + \sum_{i=1}^{n} f_i(x_i) + \sum_{1\le i<j\le n} f_{ij}(x_i, x_j) + \cdots + f_{12\ldots n}(x_1, x_2, \ldots, x_n) \tag{1}$$

where

$$\begin{aligned} &f_0 = E(y),\\ &f_i = E(y|x_i) - f_0,\\ &f_{ij} = E\left(y|x_i, x_j\right) - f_i - f_j - f_0,\\ &\ldots \end{aligned} \tag{2}$$

and so on. It shows that the original model can be decomposed into an expansion of 2^n terms of increasing dimensionality. When the input variables are independent from each other, all the terms in the right side of Eq. (1) are orthogonal and the variance of the model output can be decomposed as follows

$$V(y) = \sum_{i=1}^{n} V_i + \sum_{1\le i<j\le n} V_{ij} + \cdots + V_{12\ldots n} \tag{3}$$

Here

$$\begin{aligned} &V_i = V(E(y|x_i)),\\ &V_{ij} = V\left(E\left(y|x_i, x_j\right)\right) - V_i - V_j,\\ &\ldots \end{aligned} \tag{4}$$

and so on. By dividing both sides of Eq. (3) by the total variance $V(y)$, one obtains

$$\sum_{i=1}^{n} S_i + \sum_{1\le i<j\le n} S_{ij} + \cdots + S_{12\ldots n} = 1, \tag{5}$$

where $S_i = V_i/V(y)$, $S_{ij} = V_{ij}/V(y)$, and so on. S_i is referred to as the main effect index, or the first order effect index. It reflects the first order contribution of x_i to the output variance. S_{ij} reflects the contribution of the interaction of x_i and x_j to the output variance. Higher order terms reflect the contribution of interactions between different groups of variables.

Homma and Saltelli [26] defined total effect indices S_{Ti} as the summation of all terms including x_i, that is

$$S_{Ti} = S_i + \sum_{j=1, j\ne i}^{n} S_{ij} + \cdots + S_{12\ldots n} \tag{6}$$

Using the relationship $V(E(y|\boldsymbol{x}_{\sim i})) + E(V(y|\boldsymbol{x}_{\sim i})) = V(y)$, S_{Ti} can also be defined as [11]

$$S_{Ti} = \frac{E(V(y|\boldsymbol{x}_{\sim i}))}{V(y)} = 1 - \frac{V(E(y|\boldsymbol{x}_{\sim i}))}{V(y)} \tag{7}$$

Here $\boldsymbol{x}_{\sim i}$ denotes the vector of all input variables but x_i. $V(E(y|\boldsymbol{x}_{\sim i}))$ measures the first order contribution of $\boldsymbol{x}_{\sim i}$, and $V(y) - V(E(y|\boldsymbol{x}_{\sim i}))$ measures the contribution of all terms in the variance decomposition that include x_i.

2.2. DGSM

The idea of using derivatives to rank inputs can be traced back to the work of Morris [14], in which he introduced the notion of the elementary effects defined as the incremental ratios at given values of each input variable. Formally, for a given value of the input variable vector, denoted as $\boldsymbol{x}^*$, the elementary effect of the i-th input variables at $\boldsymbol{x}^*$, denoted as $EE_i(\boldsymbol{x}^*)$ is given by

$$EE_i(\boldsymbol{x}^*) = \frac{f\left(x_1^*, \ldots, x_i^* + \Delta, \ldots, x_n^*\right) - f(\boldsymbol{x}^*)}{\Delta} \tag{8}$$

Here Δ is a preselected increment. Under the assumption that EE_i follows distribution with a finite variance, its mean μ_i and standard deviation σ_i can be estimated as

$$\mu_i = \frac{1}{J}\sum_{j=1}^{J} EE_i\left(\boldsymbol{x}_j^*\right), \text{ and}$$
$$\sigma_i = \sqrt{\frac{1}{J}\sum_{j=1}^{J}\left(EE_i\left(\boldsymbol{x}_j^*\right) - \mu_i\right)^2} \tag{9}$$

where $\boldsymbol{x}_j^*$ is the j-th sample, and J is the total number of sampled points. The importance of the input variables can be evaluated by considering the above two statistics.

To solve the problem that positive and negative values of EE_i may cancel each other, Campolongo et al. [27] proposed a revised sensitivity index

$$\mu_i^* = \frac{1}{J}\sum_{j=1}^{J}\left|EE_i\left(\boldsymbol{x}_j^*\right)\right| \tag{10}$$

It can be seen that these sensitivity indices are based on the finite difference approximation of the derivative $\partial f/\partial x_i$ and subsequent averaging over the domain of inputs definition. It led Kucherenko et al. [13] to introduce DGSM, which was later formalized by Sobol' and Kucherenko [15] who suggested the following form of DGSM

$$\nu_i = E\left(\left(\frac{\partial f(\boldsymbol{x})}{\partial x_i}\right)^2\right) \tag{11}$$

and proved that after some normalization it is an upper bound to total effect indices S_{Ti}. Kucherenko and Ioss [28] generalized the notion of DGSM for different distributions of inputs and showed that there are also DGSM which can be lower bounds to total effect indices S_{Ti}. DGSM can be used for screening in a Factor Fixing setting [1] as their estimation is less expensive than that of the variance-based sensitivity indices.

3. The active subspace theory and activity score

3.1. The active subspace

The basic principle of active subspace theory is to find the set of most active directions in the input space. The active subspace is identified by the eigenvectors of the $n \times n$ symmetric, positive semidefinite matrix defined as follows [22]

$$\mathbf{C} = \int \nabla f(\boldsymbol{x})\nabla f(\boldsymbol{x})^{\mathrm{T}}\rho(\boldsymbol{x})d\boldsymbol{x} = \boldsymbol{W}\Lambda\boldsymbol{W}^{\mathrm{T}} \tag{12}$$

Here $\nabla f(\boldsymbol{x}) = \left(\frac{\partial f(\boldsymbol{x})}{\partial x_1}, \ldots, \frac{\partial f(\boldsymbol{x})}{\partial x_n}\right)^{\mathrm{T}}$ is the vector of gradients, $\rho(\boldsymbol{x})$ is the probability density function (PDF) of $\boldsymbol{x}$, $\boldsymbol{W} = [\mathbf{w}_1, \ldots, \mathbf{w}_n]$ is the orthogonal matrix of eigenvectors, $\Lambda = \mathrm{diag}(\lambda_1, \ldots, \lambda_n)$ is the diagonal matrix comprised by the eigenvalues which are in the descending order, i.e. $\lambda_1 \geq \ldots \geq \lambda_n$. The elements of $\boldsymbol{C}$ are the average of partial derivative products:

$$\boldsymbol{C}_{i,j} = \int \frac{\partial f(\boldsymbol{x})}{\partial x_i}\frac{\partial f(\boldsymbol{x})}{\partial x_j}\rho(\boldsymbol{x})d\boldsymbol{x} \tag{13}$$

One can see that the elements on the diagonal line of $\boldsymbol{C}$ are the DGSM defined in Eq. (11). This shows the underlying relationship between DGSM and active subspace. The following relationship holds for the eigenvalues:

$$\lambda_i = \mathbf{w}_i^{\mathrm{T}}\boldsymbol{C}\mathbf{w}_i = \int \left(\nabla f(\boldsymbol{x})^{\mathrm{T}}\mathbf{w}_i\right)^2\rho(\boldsymbol{x})d\boldsymbol{x} \tag{14}$$

It shows that if λ_i is zero, then $f(\boldsymbol{x})$ is constant along the direction defined by the eigenvector $\mathbf{w}_i$. The eigenvector matrix $\boldsymbol{W}$ defines a rotation of the original input space.

Suppose that eigenvalues are ordered in the descending order and that there is a large gap between the m-th and $(m+1)$-th eigenvalues: $\lambda_{m+1} < \lambda_m$ for some $m < n$. Consider partitioning the eigenpairs into two groups:

$$\Lambda = \begin{bmatrix}\Lambda_1 \\ \Lambda_2\end{bmatrix}, \boldsymbol{W} = [\boldsymbol{W}_1\boldsymbol{W}_2] \tag{15}$$

where $\Lambda_1 = \mathrm{diag}(\lambda_1, \ldots, \lambda_m)$, and $\boldsymbol{W}_1$ is the $n \times m$ matrix comprised by the first m eigenvector corresponding to Λ_1. If $\lambda_{m+1}, \ldots, \lambda_n$ are sufficiently small, then perturbations in the first group of coordinates cause more change of the output than perturbations in the second group of coordinates [22]. The active subspace is defined as the range of the eigenvectors in $\boldsymbol{W}_1$.

Define two vectors of new variables $\boldsymbol{u}$ and $\boldsymbol{z}$ as follows

$$\boldsymbol{u} = \boldsymbol{W}_1^{\mathrm{T}}\boldsymbol{x} \in \mathbb{R}^m, \boldsymbol{z} = \boldsymbol{W}_2^{\mathrm{T}}\boldsymbol{x} \in \mathbb{R}^{n-m} \tag{16}$$

Then $\boldsymbol{x}$ can be decomposed as

$$\boldsymbol{x} = \boldsymbol{W}\boldsymbol{W}^{\mathrm{T}}\boldsymbol{x} = \boldsymbol{W}_1\boldsymbol{W}_1^{\mathrm{T}}\boldsymbol{x} + \boldsymbol{W}_2\boldsymbol{W}_2^{\mathrm{T}}\boldsymbol{x} = \boldsymbol{W}_1\boldsymbol{u} + \boldsymbol{W}_2\boldsymbol{z}. \tag{17}$$

The original input-output function can be approximated as

$$f(\boldsymbol{x}) = f(\boldsymbol{W}_1\boldsymbol{u} + \boldsymbol{W}_2\boldsymbol{z}) \approx f(\boldsymbol{W}_1\boldsymbol{u}) = g(\boldsymbol{u}) \tag{18}$$

Here the original model is rebuilt in the reduced (or active) subspace. We refer to $\boldsymbol{u}$ as the vector of active variables.

3.2. Activity score

Using the theory of active subspaces, Constantine and Diaz [25] introduced the so-called activity score defined as

$$a_i = \sum_{j=1}^{m}\lambda_j w_{i,j}^2 i = 1, \ldots, n \tag{19}$$

where a_i denotes the activity score of x_i, and $w_{i,j}$ denotes the ith component of the jth eigenvector corresponding to an eigenvalue λ_j. In Section 3.1, the active subspace was defined by the first m eigenvalues and eigenvectors. The activity score is a combined reflection of the contribution of each input variable to the active subspace. The corresponding element of x_i in $\mathbf{w}_j$, i.e. $w_{i,j}$, reflects the relative change of x_i in the direction defined by $\mathbf{w}_j$. Thus $w_{i,j}$ is a measure of the significance of x_i in this direction. Squaring $w_{i,j}$ removes the effects of signs similarly to the definition of DGSM in Eq. (11).

The activity score can be viewed as a byproduct of finding active subspace for model reduction. It can be used to rank the importance of input variables according to their contributions to the active subspace. Constantine and Diaz [25] established a link between the activity score and DGSM

$$a_i(m) \leq \nu_i \tag{20}$$

Here m denotes the number of considered eigenvectors. Inequality becomes the equality at $m = n$. The total effect index is bounded as follows [25]

$$S_{Ti} \leq \frac{1}{4\pi V(y)}\left(a_i(m) + \lambda_{m+1}\right) \tag{21}$$

where λ_{m+1} is the $m+1$th eigenvalue. For some models, the three GSA indices give similar importance rankings of the input variables, meaning that one can select the index which is easier to compute. Sobol' and Kucherenko [15] pointed out that for highly nonlinear functions the ranking of important variables using DGSM may be different from that based on total effect indices.

4. A GSA approach based on active subspace and Kriging surrogate metamodeling

Surrogate models such as Kriging are used as an approximation of real models to alleviate the computational burden. The convergence speed of building Kriging may become very low with the increase of input dimensions. For many problems the model output largely depends on relatively few directions in the input space. Methodologies such as active subspaces allow model reduction by building the surrogate model in the active subspace instead of the whole input space [29].

In this section, we present an integrated procedure which allows to estimate the three GSA indices: activity score, DGSM and Sobol' total effect indices within a single loop of analysis. The flowchart of the proposed approach is shown in Fig. 1. Each step of the procedure is also explained in detail.

Step 1: Generate the full sample set S_0.

Generate a set with N_0 samples using an efficient sampling technique such as e.g. low discrepancy Sobol' sequences [30–32]. All the inputs are preliminary normalized into the [-1, 1] interval. The sample set is denoted as S_0.

Step 2: Estimate the matrix $\boldsymbol{C}$ and DGSM.

Draw N_1 samples from S_0, and scale down these samples. The generated sample set is denoted as S_1. Estimate $\nabla f(\boldsymbol{x})$ at these samples by the finite difference or adjoint algorithmic differentiation (AAD) methods [33]. Estimate the elements of matrix $\boldsymbol{C}$ by averaging the gradients at these sampled points. On this step, the DGSM are also obtained using the diagonal elements of $\boldsymbol{C}$.

Step 3: Perform the eigenvalue decomposition and identify the active subspace.

Obtain the eigenvalues and eigenvectors by the eigenvalue decomposition of the matrix $\boldsymbol{C}$. The active subspace can be identified by analyzing the relative distances between eigenvalues. Compute the activity score index.

Step 4: Build Kriging surrogate model in the active subspace.

The Kriging surrogate model is built by an adaptive sample selection process.

Step 5: Estimate total effect indices.

Total effect indices are estimated using MC or QMC estimators by calling the Kriging model instead of the original model.

4.1. Discussion of Step 1

On this step the advanced sampling techniques based on Latin hypercube sampling [30] or Sobol' sequences [31] are used to draw the initial sample set. These sampling techniques are designed to sample in the unit hypercube as uniformly as possible. The normalization to the

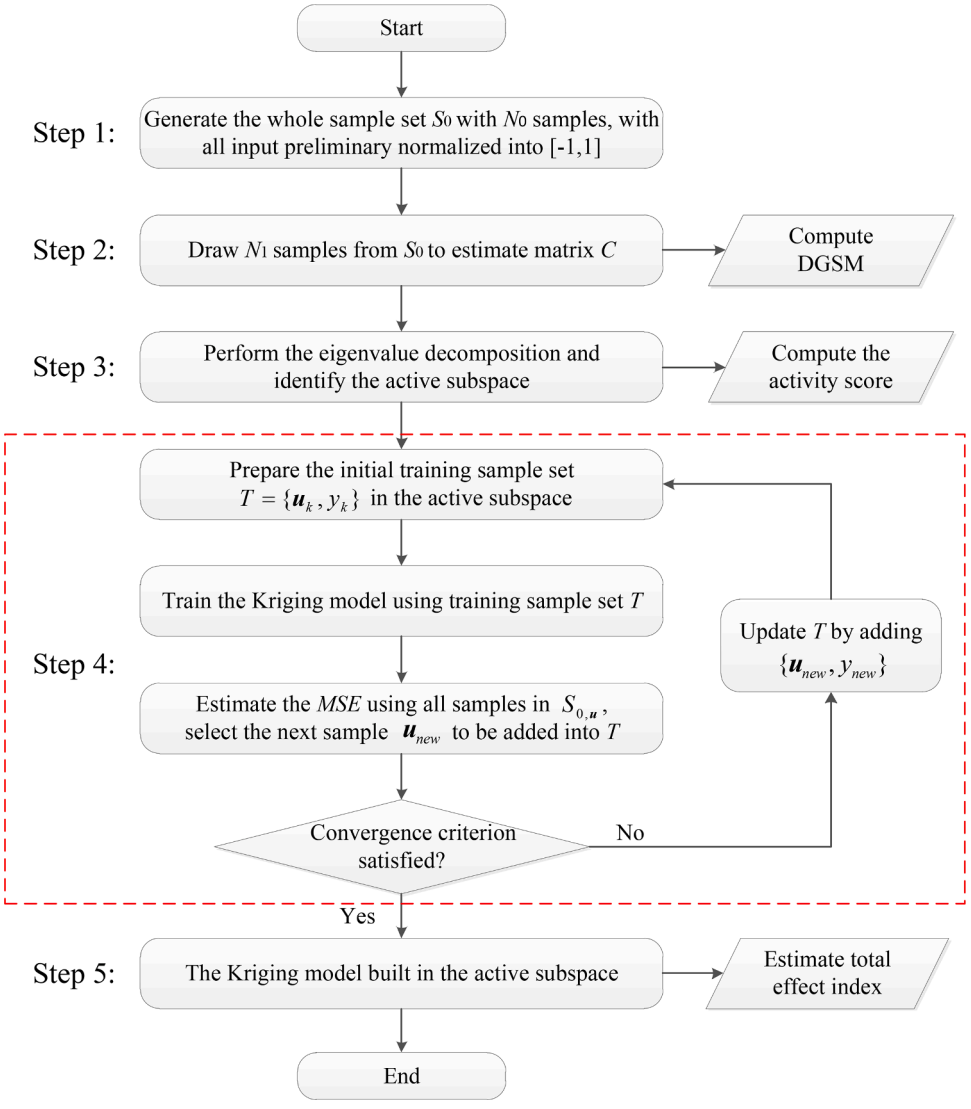

Fig. 1. Flowchart of the proposed approach.

interval [-1, 1] removes possible various scaling of inputs [22]. However, when computing the corresponding model outputs, the normalized samples must be transformed to the original space before being substituted into the model.

4.2. Discussion of Step 2

The first-order finite difference method is used in this work for estimating gradients:

$$\frac{\partial f(\boldsymbol{x})}{\partial x_i} \approx \frac{f(\boldsymbol{x}_{\sim i}, x_i + h) - f(\boldsymbol{x})}{h} \tag{22}$$

Here h is the increment (step size), and $\boldsymbol{x}_{\sim i}$ is the vector of all input variables but the input x_i. Other algorithms can be also used for estimating gradients. The most efficient of such algorithms with respect to the number of required model evaluation is AAD [33]. Constantine [22] also shows that in some cases it is possible to fit the original model by local or global linear functions and then to compute the gradients. He pointed out that eigenvalues smaller than h are estimated less accurately than those larger than h. In this work, the value of h is taken as 1×10^{-5}.

To enhance the accuracy and efficiency, a strategy of scaling is introduced during this step. According to Peng [34], proper scaling of the input space to smaller spaces can reduce the error and the required number of samples to estimate the averaged gradients. He suggested using the value of the scaling factor between 0.01 and 0.001. A scaling factor which is smaller than 1 is introduced and denoted by β. The drawn samples are then multiplied by the scaling factor β, and the scaled sample pool is denoted by S_1, i.e., $S_1 = \{\beta \boldsymbol{x}_j, j = 1,\ldots,N_1\}$. In test cases of this work, the scaling factor is taken to be equal 0.01.

After estimation of gradients the matrix $\boldsymbol{C}$ is computed as

$$\boldsymbol{C} \approx \widehat{\boldsymbol{C}} = \frac{1}{N_1}\sum_{j=1}^{N_1} \nabla f(\beta \boldsymbol{x}_j) \nabla f(\beta \boldsymbol{x}_j)^{\mathrm{T}} = \widehat{\boldsymbol{W}}\widehat{\Lambda}\widehat{\boldsymbol{W}}^{\mathrm{T}} \tag{23}$$

To improve the efficiency, Constantine and Gleich [35] suggested choosing the value of N_1 according to the following criterion:

$$N_1 = \alpha m \log(n) \tag{24}$$

where α is an oversampling factor with a recommended value to be chosen between 2 and 10, m is the estimated dimension of the active subspace, and n is the dimension of the original input space. The computational cost of estimating the matrix $\boldsymbol{C}$ using the finite difference method is $N_1(n+1)$. DGSM indices being the diagonal elements of $\boldsymbol{C}$ are also computed on this step.

4.3. Discussion of Step 3

On this step we perform the decomposition of the estimate $\widehat{\boldsymbol{C}}$ to obtain the eigenvalues and eigenvectors using the singular value decomposition (SVD) method [36]. As discussed in Section 3.1, the dimension of the active subspace can be identified by comparing the eigenvalues ranked in the descending order. Constantine [22] suggested comparing the gaps between the eigenvalues: a large gap in the eigenvalues indicates the boundary between the active and inactive subspaces. If $\lambda_{m+1}, \ldots, \lambda_n$ are sufficiently small, then the active subspace is defined by the first m eigen vectors.

After finding the active subspace, the mapping between the original input variables $\boldsymbol{x}$ and the variables $\boldsymbol{u}$ in the active subspace is approximated as

$$\boldsymbol{x} = \boldsymbol{W}_1\boldsymbol{u} + \boldsymbol{W}_2\boldsymbol{z} \approx \boldsymbol{W}_1\boldsymbol{u} \tag{25}$$

where $\boldsymbol{u}$ and z are called the vector of active variables and inactive variables, respectively.

On this step, the activity score can be obtained using definition in Eq. (19).

4.4. Discussion of Step 4

As the original model $f(\boldsymbol{x})$, is now approximated by the model within the active subspace, i.e. $g(\boldsymbol{u})$ we can build the Kriging surrogate model of $g(\boldsymbol{u})$ instead of $f(\boldsymbol{x})$. It should be easier than building a surrogate model for $f(\mathbf{x})$ as the dimension is reduced. We choose Kriging in this work because not only it is capable of interpolating the response surface from a limited number of data points but it can also provide the mean squared error (*MSE*) as an estimate of the prediction error on an unobserved point. The *MSE* is used in the criteria for selecting new samples and evaluating the convergence. The general principle of Kriging is briefly reviewed in the Appendix. The procedure of adaptively building the Kriging model in the active subspace is as follows:

Substep 1: Map all the samples in S_0 to the active subspace $\boldsymbol{u}$ using relationship in Eq. (25). The new sample set is denoted $S_{0,\boldsymbol{u}}$. For $k = 1,\ldots, N_2$, draw $\boldsymbol{u}_k$ from $S_{0,\boldsymbol{u}}$ and obtain the corresponding model outputs y_k. Note that $\boldsymbol{u}_k$ must be firstly transformed to $\boldsymbol{x}_k$, and then transformed to the original inputs before being substituted into the original model (we recall that the samples are normalized into the interval [-1, 1] in Section 4.1). Thus the initial training data set $T = \{\boldsymbol{u}_k, y_k\}$ is formed.

Substep 2: Train the Kriging model, denoted as $\widehat{g}(\boldsymbol{u})$, with the training data set T.

Substep 3: Use the surrogate model $\widehat{g}(\boldsymbol{u})$ to estimate *MSE* for all samples in $S_{0,\boldsymbol{u}}$. Identify the sampled point with the largest *MSE*:

$$\boldsymbol{u}_{new} = \underset{\boldsymbol{u}\in S_{0,\boldsymbol{u}}}{arg\max} MSE \tag{26}$$

Substep 4: Check the convergence of the Kriging model. This is done by comparing the maximum *MSE* at adjacent iterations. The convergence criterion is defined as

$$\left|\frac{\max MSE^{l} - \max MSE^{l-1}}{\max MSE^{l-1}}\right| \le Cr \tag{27}$$

where $\max MSE^{l}$ and $\max MSE^{l-1}$ denote the maximum *MSE* of all samples in $S_{0,\boldsymbol{u}}$ at the ith and $(l-1)$-th iterations, with $l > 1$. In this work the value of Cr is taken to be equal to 5×10^{-4}. When Eq. (27) does not hold, $\boldsymbol{u}_{new}$ is mapped into the original input space, and the corresponding model output y_{new} is obtained by calling the original model. Then the new training point $\{\boldsymbol{u}_{new}, y_{new}\}$ is added into T for update and training on Substep 2 is renewed. If Eq. (27) holds, the Kriging model is considered to be sufficiently accurate.

4.5. Discussion of Step 5

On this step, Sobol' total effect indices is estimated. By the Kriging model $y = \widehat{g}(\boldsymbol{u})$ the direct simulation methods to compute the index can be used. In this work we use estimators presented in Refs. [11,37].

In summary, the estimates of the three types of GSA indices are integrated into a single loop of analysis. The computational cost is measured by the number of calls to the original model, and it consists of two parts. The first part comes from the estimate of $\boldsymbol{C}$ on Step 2, which requires $N_1(n+1)$ calls of the real model. The second part comes from the training of Kriging model in the active subspace, which requires $N_2 + N_3$ model calls, where N_2 is the number of initial training samples, and N_3 denotes the number of adaptively added training samples. Thus, the total computational cost of the proposed approach is $N_1(n+1) + N_2 + N_3$. We note that computational costs of the first part can be dramatically decreased to only $(4 \sim 6)N_1$ model calls if AAD methods are used to compute derivatives [33]. The proposed approach can be applied for other tasks such as reliability analysis, uncertainty based optimization, etc.

5. Validation test cases

In this section, GSA based on the proposed approach is performed on five test cases. As the primary purpose of GSA is to rank the importance of input variables, the three sensitivity indices are normalized for fair comparison following Constantine and Diaz [25]. For a sensitivity index γ_i the normalized version is expressed as

$$\overline{\gamma}_i = \frac{\gamma_i}{\left(\sum_{i=1}^{n} \gamma_i^2\right)^{1/2}} \tag{28}$$

In the examples discussed in the following, all GSA indices are normalized according to Eq. (28).

To quantitatively show the accuracy level of the built Kriging model, the relative mean square error (*RMSE*) and the relative maximum absolute error (*RMAE*) defined as [24]

$$RMSE = \sum_{i=1}^{N} \left(f^{(i)} - \widehat{g}^{(i)}\right)^2 \Big/ \sum_{i=1}^{N} \left(f^{(i)} - \overline{f}^{(i)}\right)^2 \tag{29}$$

$$RMAE = \frac{1}{STD} \max\left|f^{(i)} - \widehat{g}^{(i)}\right| \tag{30}$$

$$STD = \sqrt{\frac{1}{N-1} \sum_{i=1}^{N} \left(f^{(i)} - \overline{f}^{(i)}\right)^2} \tag{31}$$

are estimated for each test case. Here $f^{(i)}$ (i=1,…,N) denotes the i-th observation of true model value, $\widehat{g}^{(i)}$ is the corresponding Kriging model in the active subspace, $\overline{f}^{(i)}$ is the mean value of $f^{(i)}$, and N is the total number of test samples.

For comparison purposes the three GSA indices are computed also by MCS. For the DGSM and activity score, similarly to Eq. (23), the matrix $\boldsymbol{C}$ is estimated as follows

$$\mathbf{C} \approx \widehat{\mathbf{C}} = \frac{1}{N_{\mathrm{MC}}} \sum_{j=1}^{N_{\mathrm{MC}}} \nabla f(\mathbf{x}_j) \nabla f(\mathbf{x}_j)^{\mathrm{T}} = \widehat{\mathbf{W}} \widehat{\Lambda} \widehat{\mathbf{W}}^{\mathrm{T}} \tag{32}$$

To keep the credibility of MCS, neither Eq. (24) nor the scaling technique in Section 4.2 are used here to determine the value of N_{MC}. N_{MC} can be large enough to ensure the accuracy of MCS. $\nabla f(\boldsymbol{x}_j)$ is estimated by the finite difference method. Thus, the total computational cost for estimating the DGSM and activity score is $N_{\mathrm{MC}}(n+1)$. The strategy proposed by Jansen [37] is used to estimate total effect indices, which requires $N_{\mathrm{MC}}(n+1)/2$ calls to the original model, in which $N_{\mathrm{MC}}/2$ calls can be saved by reusing the samples from estimating matrix $\boldsymbol{C}$ in Eq. (32). Thus, the total computational cost of MCS is $N_{\mathrm{MC}}(3n/2+1)$.

It needs to be pointed out that there should exist an optimal value of N_{MC}, which may be found by performing a convergence analysis. Furthermore, the sample size of MCS for estimating the DGSM and activity score can be different from that for estimating total effect indices. As the focus of this work is to discuss building surrogate model in reduced dimensions and its application in sensitivity analysis, the role of MCS is to offer a reliable reference result to justify the correctness and to show the efficiency of the proposed approach. Thus, in this work we are using a large value of N_{MC}, provided that the computational cost is affordable. Finding an optimal sample size for MCS needs a special and comprehensive study like Ref. [11], and it can be done separately in the future.

5.1. Example 1: a quadratic function

In this example, a quadratic function without crossing terms is considered

$$y = -15x_1 + 2x_1^2 - 3x_2 + x_2^2 + 5x_3 + x_3^2 + 40 \tag{33}$$

Here all the input variables follow the standard normal distribution.

Firstly, a total of 1×10^5 samples are drawn as the full sample set. Then N_1 is used to estimate $\boldsymbol{C}$. The oversampling factor α is taken as 2 in this work. The value of m depends on the dimension of active subspaces. As the model dimension in this example is only 3, we take $m = 3$. Then, according to Eq. (24), $N_1 = 6$. These sampled inputs are further scaled by multiplying by the scaling factor 0.01. With the finite difference method, $6 \times (3+1) = 24$ model runs are needed to estimate the average gradients in $\boldsymbol{C}$. The decomposition of $\boldsymbol{C}$ is performed by SVD. The eigenvalues arranged in the descending order are 227, 10.1, and 2.03. There is an obvious gap between the first and second eigenvalue, which implies that there exists a one-dimensional active subspace. Thus, we construct the surrogate model based on the first eigenvalue and the corresponding eigenvector. Following Step 4 of the proposed approach, 200 samples are drawn to train the Kriging model. Then 118 samples are adaptively selected to update the Kriging model until the convergence criterion is reached. The final value of Cr is 2.19×10^{-4}. The number of samples for building the Kriging model is $200 + 118 = 318$. Sampled points used in the adaptive training process and the Kriging model in the active subspace are shown in Fig. 2. The *RMSE* and *RMAE* of the Kriging model are 0.0195 and 1.3223, respectively. It shows that the Kriging model built in the active subspace can accurately approximate the real model with a modest computational cost.

The three normalized sensitivity indices estimated by the proposed approach and MCS are shown in Table 1. It can be seen that the values of sensitivity measures obtained by the proposed approach agree well with the MCS solutions, which demonstrates high efficiency of the proposed approach. The total number of model runs is $318 + 24 = 342$. For MCS, this number is 5.5×10^5 with $N_{\mathrm{MC}} = 1 \times 10^5$. The normalized values of the three GSA indices are similar to each other.

5.2. Example 2: a high-dimensional quadratic model

A high-dimensional quadratic model is considered:

$$y = \left(\sum_{i=1}^{100} c_i x_i\right)^2 \tag{34}$$

Here $x_i, i = 1, \ldots, 100$ follow the uniform distribution on [0, 1], and the values of coefficients c_i are given in Table 2. In this example the importance of the input variables depends on their coefficients: a larger coefficient means higher importance of the corresponding input

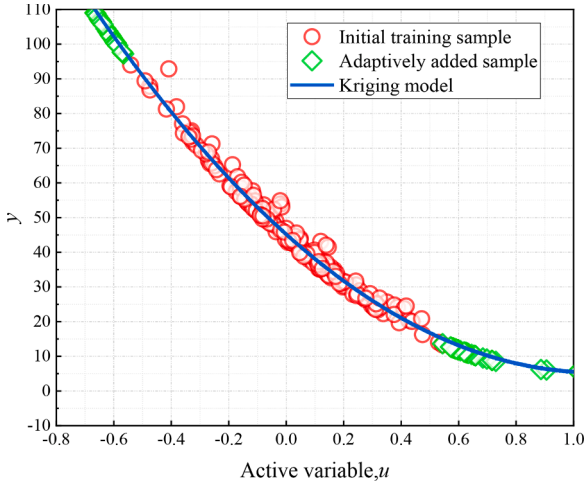

Fig. 2. The training samples and Kriging model in the active subspace of Example 1.

Table 1
The normalized GSA indices in Example 1.

Input variable	Proposed approach			MCS		
	DGSM	Activity score	Total effect indices	DGSM	Activity score	Total effect indices
x_1	0.9911	0.9911	0.9899	0.9943	0.9952	0.9921
x_2	0.0391	0.0391	0.0441	0.0366	0.0333	0.0471
x_3	0.1272	0.1272	0.1348	0.1006	0.0916	0.1157

Table 2
Values of the coefficients in Example 2.

c_5	c_{15}	c_{25}	c_{35}	c_{45}	c_{55}	c_{65}	c_{75}	c_{85}	c_{95}	The rest
5	15	25	35	45	55	65	75	85	95	1

variable. We use this example to test the applicability of the proposed approach in high-dimensional cases.

A total of 1×10^5 samples are drawn using Latin hypercube sampling. Value of $\alpha = 2$ was taken to decide the value of N_1. There are many studies in the literature showing that typically the dimension of the active subspace is not higher than two [22,24,25]. Considering the constraints on the computational cost, we take $m = 5$, which means at least 5 eigenvalues larger than 0 can be obtained [35]. Then based on Eq. (24) $N_1 = 46$, thus a total number of model calls to get the estimate of $\boldsymbol{C}$ is $46 \times (100 + 1) = 4646$. The decomposition of $\boldsymbol{C}$ is performed by SVD. According to the active subspace theory, the gap in the eigenvalues indicates a separation between active and inactive subspaces. To find such gaps, we plot the eigenvalues in Fig. 3. Note that eigenvalues change sharply, thus they are plotted on a logarithmic scale.

The large gap between the first and the second eigenvalue implies that there exists one-dimensional active subspace. The Kriging model is built in the active subspace. 200 samples are selected as the initial training data. On the adaptive training step, further 32 samples are added to update the Kriging model, and the whole process converges at $Cr = 4.48 \times 10^{-4}$. The sample points and the Kriging model in the active subspace are shown in Fig. 4(a). The *RMSE* and *RMAE* of the Kriging model built are 2.86×10^{-14} and 8.06×10^{-7}, respectively. For comparison, the Kriging model is also built in the two-dimensional active subspace as shown in Fig. 4(b). It can be noticed that the Kriging model built in one-dimensional active subspace is sufficient to capture the general behavior of output, and that in two-dimensional active subspace adds little information. We will also compare the results of the proposed approach by considering one-dimensional and two-dimensional active subspaces.

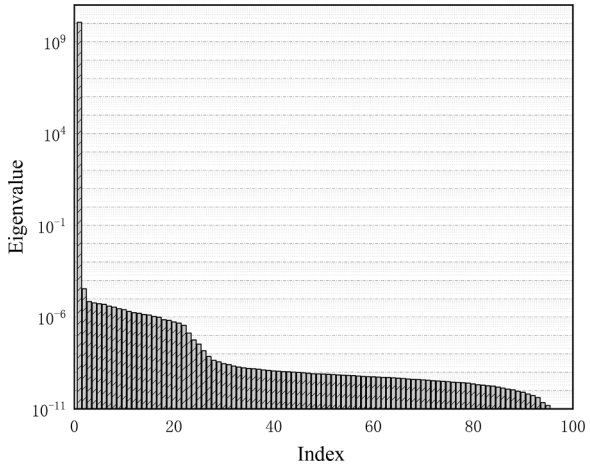

Fig. 3. The eigenvalues in Example 2.

The three GSA indices of all the input variables obtained by the proposed approach (in one-dimensional active subspace) as well by MCS are presented in Fig. 5. The results obtained by the proposed approach agree well with those obtained by MCS, which proves that the proposed approach is applicable in the high-dimensional case. Normalized values of DGSM and activity score are almost the same as the values of total effect indices. Computed GSA indices have successfully quantified the importance of the input variables: $x_{95} > x_{85} > x_{75} > x_{65} > x_{55} > x_{45} > x_{35} > x_{25} > x_{15} > x_5 >$ other inputs. The total number of model runs by the proposed approach is $4646 + 200 + 32 = 4878$. The computational cost of the approach in this high-dimensional example is relatively high compared to that in Example 1 due to the cost of estimating the matrix $\boldsymbol{C}$ in high dimensions. Thus, more efficient algorithms for estimating the matrix $\boldsymbol{C}$ in high-dimensional cases need further development.

For illustration, the GSA indices of the first 10 most important input variables are presented in Fig. 6. The proposed approach is applied by building the Kriging model in one-dimensional active subspace (1D) and two-dimensional active subspace (2D), respectively. We also build the Kriging model by the criterion in Section 4.4 in the original whole input space, and then estimate total effect indices. As the DGSM results are obtained after the matrix $\boldsymbol{C}$ is obtained, only MCS and the proposed approach (1D or 2D) are compared. For the activity score and total effect indices, when using the proposed approach there is practically no difference between the results obtained in one- and two-dimensional active subspaces (Fig. 4). For total effect indices, the results obtained by directly building the surrogate model in the original input space (black bars in Fig. 6) deviate from the other methods: black bars do not match those corresponding to the proposed approach and MCS. This conventional approach needs 200 + 67 training points, which is more than required by the proposed approach (232 function calls).

We have also tested the application of the proposed approach in this example when the input variables follow different types of distributions. As the importance of the input variables depends only on their coefficients in Eq. (34), we only list representative indices of the proposed approach, that is, the number of added samples, *RMSE* and *RMAE*. The results are shown in Table 3. Small values of these indices confirm that the proposed approach is applicable for all considered distribution types. It confirms also that there is no constraint on the distribution type of input variables in the procedure of the proposed approach and it can be used for different probabilistic distributions.

5.3. Example 3: a cylindrical piston model

We study a cylindrical piston model which has been used by researchers to test parameter screening techniques [25]. The model output t is the time in seconds that it takes to complete one cycle. It is obtained according to the following system of equations:

$$t = 2\pi\sqrt{\frac{M}{k + S^2\frac{P_0V_0}{T_0}\frac{T_a}{V^2}}} \tag{35}$$

$$V = \frac{S}{2k}\left(\sqrt{A^2 + 4k\frac{P_0V_0}{T_0}T_a} - A\right) \tag{36}$$

$$A = P_0S + 19.62M - \frac{kV_0}{S} \tag{37}$$

where the input variables follow the uniform distribution. The distribution parameters are shown in Table 4.

Similar to the steps in the first two examples, we set $\alpha = 2$ and $m = 5$, then $N_1 = 19$ according to Eq. (24). The estimate of $\boldsymbol{C}$ takes $19 \times (7 + 1) = 152$ model runs. The eigenvalues obtained by the decomposition of $\boldsymbol{C}$ are plotted in Fig. 7. Obviously, there is a gap in the first eigenvalue and the rest, thus the active subspace in this test case is one-dimensional. In the active subspace, 200 samples are selected as the initial training data

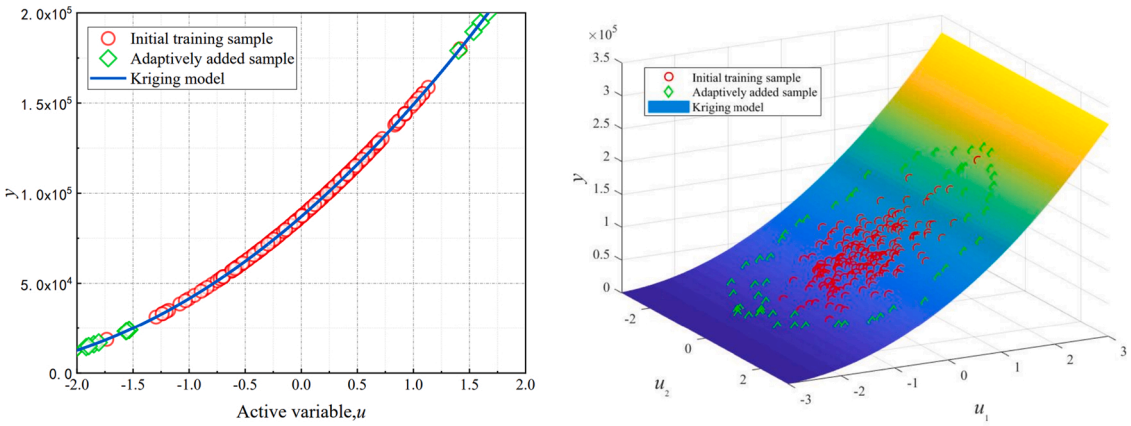

(a) One-dimensional active subspace (b) Two-dimensional active subspace

Fig. 4. The training samples and Kriging model in the active subspace of Example 2.

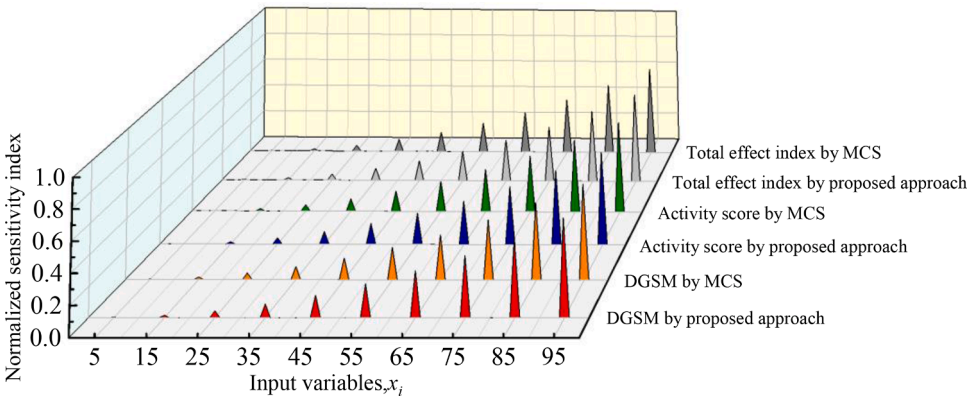

Fig. 5. GSA indices in Example 2.

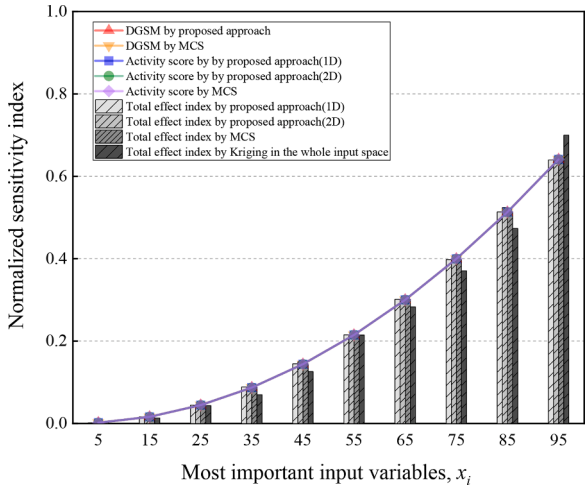

Fig. 6. The GSA indices for the most important input variables in Example 2.

and 167 new samples are added on the adaptive step. The training samples and the Kriging model in the active subspace is shown in Fig. 8. The final value of *Cr* is 1.51×10^{-4}. The *RMSE* and *RMAE* of the built Kriging model are 0.0127 and 0.8084, respectively.

The GSA indices obtained by the proposed approach, as well as the results obtained by the direct MCS, are shown in Fig. 9. The total computational cost by the proposed approach is $152 + 200 + 167 = 519$ model runs, while the cost of MCS is 1.15×10^6 with $N_{MC} = 1 \times 10^5$. The proposed approach gives almost the same estimates of the sensitivity indices as the MCS. The three GSA indices give the same importance ranking of the input variables in the descending order of importance: {*S*, V_0, *M*, *k*, P_0, T_a, T_0}.

5.4. Example 4: a ten-bar structure

We consider a ten-bar structure [38] shown in Fig. 10. The length of each horizontal and vertical bar is *L*, the sectional area is A_i ($i = 1,\ldots,10$), and the elastic modulus is *E*. P_1, P_2 and P_3 are the external loads. Inputs *L*, A_i ($i = 1,\ldots,10$), *E*, P_1, P_2, P_3 follow the normal distribution with parameters given in Table 5. We consider the vertical displacement at Node 2 as the quantity of interest and study the contribution of input variables to the output uncertainty using GSA.

In this example, we set $\alpha = 2$ and $m = 5$, which gives $N_1 = 27$ according to Eq. (24). $27 \times (15 + 1) = 432$ model runs are used to estimate the matrix $\boldsymbol{C}$. The eigenvalues obtained by the decomposition of $\boldsymbol{C}$ are plotted in Fig. 11, from which it is clear that the active subspace is one-dimensional. Upon the initially selected 200 samples for building the Kriging model, another 43 samples are added to update the Kriging model. The Kriging model as well as the training samples are shown in Fig. 12. The final value of *Cr* is 3.18×10^{-4}. The *RMSE* and *RMAE* of the built Kriging model are 0.0159 and 1.9640, respectively.

The GSA indices obtained by the proposed approach and MCS are shown in Fig. 13. The computational cost of the proposed approach and MCS are $432 + 200 + 43 = 675$ and 2.35×10^6 with $N_{MC} = 1 \times 10^5$,

Table 3
Application of the proposed approach with different distributions.

Distribution	Parameter *A*	Parameter *B*	Value of *A*	Value of *B*	number of added samples	*Cr*	*RMSE*	*RMAE*
Gamma	shape parameter	scale parameter	1	1	16	1.5×10^{-4}	1.4×10^{-13}	7.9×10^{-6}
Beta	first shape parameter	second shape parameter	1	1	270	1.1×10^{-4}	2.9×10^{-14}	7.4×10^{-7}
Poisson	mean	/	1	/	14	8.3×10^{-5}	3.5×10^{-14}	4.1×10^{-6}
Exponential	mean	/	1	/	123	4.3×10^{-4}	2.7×10^{-4}	7.2×10^{-6}
Lognormal	mean of logarithmic values	standard deviation of logarithmic values	1	1	278	2.2×10^{-4}	4.8×10^{-12}	4.3×10^{-5}

Table 4
Input variables in the piston model.

Inputs	Notation	Units	Minimum	Maximum
Weight	M	kg	30	60
Surface area	S	m^2	0.005	0.020
Initial gas volume	V_0	m^3	0.002	0.010
Spring coefficient	k	N/m	1000	5000
Atmospheric pressure	P_0	N/m^2	90000	110000
Ambient temperature	T_a	K	290	296
Filling gas temperature	T_0	K	340	360

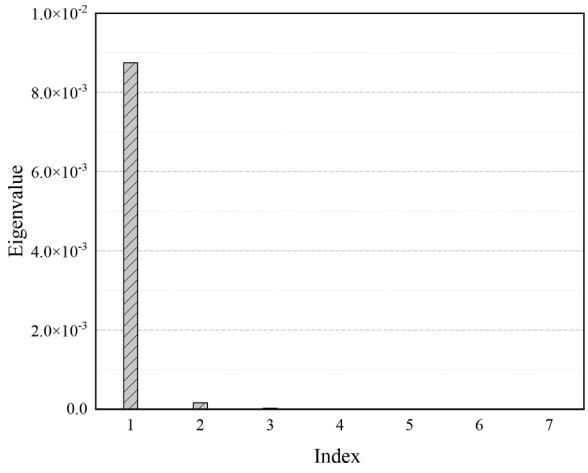

Fig. 7. The eigenvalues in Example 3.

respectively. The GSA indices give the relative contribution of the input variables to the uncertainty of the displacement at Node 2. It shows that L, A_1, A_3, A_7, A_8, E, P_1, P_2 have obvious impacts. In fact, this conclusion can be justified by a qualitative study based on the mechanics of materials. The displacement at Node 2 is caused by the deformation of each bar under axial tension and compression, and the deformation is positively proportional to the length and negatively proportional to the elastic modulus, thus L and E should be important. As the output of interest is a vertical displacement, it is understandable that the horizontal load P_3 has little impact on it. It can also be judged by the mechanics of materials that those bars (including A_1, A_3, A_7, A_8) close to the restrained end (on the left) are more important to the vertical displacement at Node 2 than those bars close to the unrestrained end (on the right).

5.5. Application case: safety analysis of a radome structure

The radome structure is used in aircrafts to protect the antenna or radar on board against external loads or lighting strikes. The fiber reinforced composites are widely used as the material of radome due to

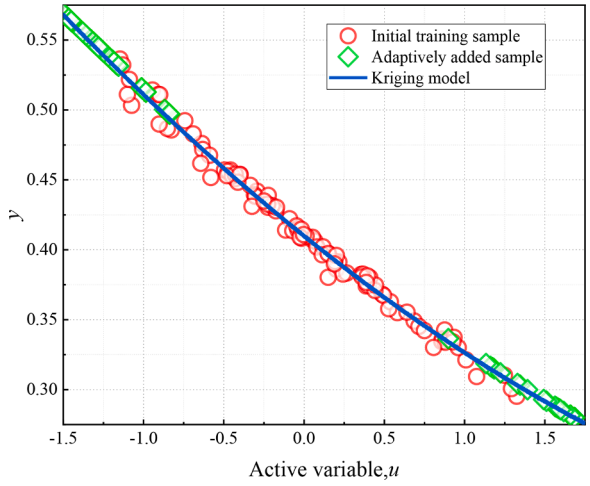

Fig. 8. The training samples and Kriging model in the active subspace of Example 3.

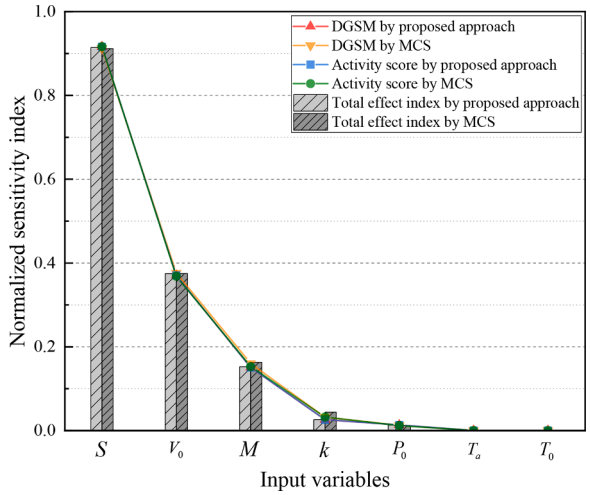

Fig. 9. GSA indices in Example 3.

the characteristic of lightness and high strength. The finite element analysis (FEA) model of the radome structure is shown in Fig. 14. The radome is fixed to the fuselage at three joints, and is subject to aerodynamic loads.

Uncertainties widely exist in the manufacturing of composite materials. In this application case, a total of 17 input variables are considered, their distribution information is shown in Table 6.

In this application, the first-ply failure assumption and the Tsai-Wu criterion are adopted to consider the safety of the radome. The crite-

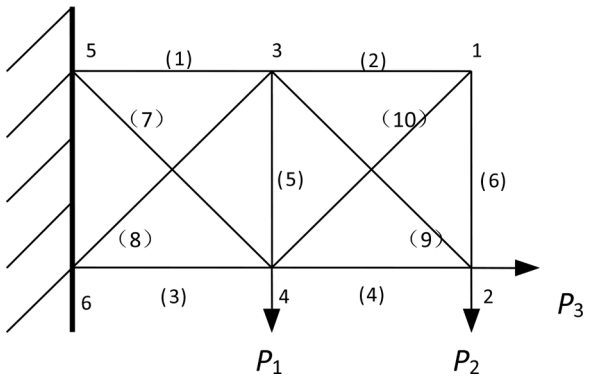

Fig. 10. A ten-bar structure.

Table 5
Values of parameters in the ten-bar structure.

Input variable	L	A_i	E	P_1	P_2	P_3
Mean	1 m	0.001 m^2	100 GPa	80 kN	10 kN	10 kN
Coefficient of variation	0.05	0.15	0.05	0.05	0.05	0.05

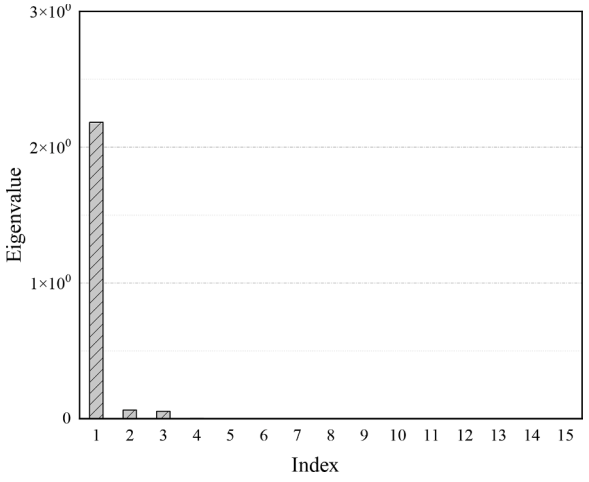

Fig. 11. The eigenvalues in Example 4.

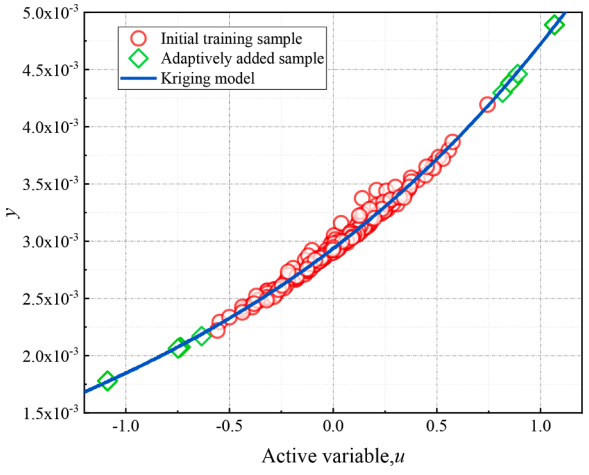

Fig. 12. The training samples and Kriging model in the active subspace of Example 4.

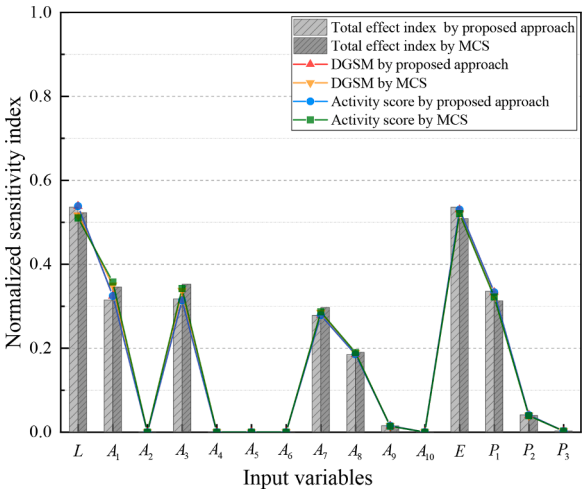

Fig. 13. GSA indices in Example 4.

Fig. 14. FEA model of the radome structure.

Table 6
Distribution information of input variables of the composite radome.

Variable	Mean	Standard deviation	Distribution type
Elastic modulus in 11th direction E_{11} (Pa)	4.9×10^{10}	4.9×10^{9}	Normal
Elastic modulus in 22nd direction E_{22} (Pa)	1.3×10^{10}	1.3×10^{9}	Normal
Elastic modulus in 12th direction G_{12} (Pa)	4.4×10^{9}	4.4×10^{8}	Normal
Elastic modulus in 13th direction G_{13} (Pa)	3.6×10^{9}	3.6×10^{8}	Normal
Elastic modulus in 23rd direction G_{23} (Pa)	2.7×10^{9}	2.7×10^{8}	Normal
0 degree ply angle *Ang_0*	0°	4.5 °	Normal
90 degree ply angle *Ang_90*	90°	4.5 °	Normal
45 degree ply angle *Ang_45*	45°	4.5 °	Normal
-45 degree ply angle *Ang_-45*	-45°	4.5 °	Normal
Thickness of single-layer plate m (m)	1.5×10^{-4}	1.5×10^{-5}	Normal
Material density ρ(kg/m^3)	1400	140	Normal
Longitudinal tensile strength X_t (Pa)	1.5×10^{9}	1.5×10^{8}	Normal
Longitudinal compressive strength X_c (Pa)	6.8×10^{8}	6.8×10^{7}	Normal
Transverse tensile strength Y_t (Pa)	4.1×10^{8}	4.1×10^{7}	Normal
Transverse compressive strength Y_c (Pa)	2.0×10^{8}	2.0×10^{7}	Normal
In-plane shear strength S (Pa)	9.5×10^{7}	9.5×10^{6}	Normal
Interlaminar shear strength S_b (Pa)	1.0×10^{8}	1.0×10^{7}	Normal

rion is given as [39]

$$F_1\sigma_1 + F_2\sigma_2 + F_{11}\sigma_1^2 + F_{22}\sigma_2^2 + 2F_{12}\sigma_1\sigma_2 + F_{66}\sigma_6^2 = 1 \tag{38}$$

where $F_1 = \frac{1}{X_t} - \frac{1}{X_c}$, $F_2 = \frac{1}{Y_t} - \frac{1}{Y_c}$, $F_{11} = \frac{1}{F_1F_2}$, $F_{22} = \frac{1}{Y_tY_c}$, $F_{66} = \frac{1}{S^2}$, $F_{12} = \frac{I}{\sqrt{X_tX_cY_tY_c}}\sigma_1$, σ_2 and σ_6 can be obtained by FEA, and the coefficient I is taken to be equal to -0.5.

The Tsai-Wu strength ratio (SR) is defined as

$$SR = \frac{\{\sigma_{\max}\}}{\{\sigma\}} \tag{39}$$

where $\{\sigma_{\max}\}$ and $\{\sigma\}$ denote the strength and stress, respectively. When considering the limit state of failure of the composite structure Eq. (38) becomes

$$F_1\sigma_{\max,1} + F_2\sigma_{\max,2} + F_{11}\sigma_{\max,1}^2 + F_{22}\sigma_{\max,2}^2 + 2F_{12}\sigma_{\max,1}\sigma_{\max,2} + F_{66}\sigma_{\max,6}^2 = 1 \tag{40}$$

Substituting Eq. (39) into Eq. (40), we obtain

$$F_1SR\sigma_1 + F_2SR\sigma_2 + F_{11}SR^2\sigma_1^2 + F_{22}SR^2\sigma_2^2 + 2F_{12}SR^2\sigma_1\sigma_2 + F_{66}SR^2\sigma_{12}^2 - 1 = 0 \tag{41}$$

Solving this equation for SR:

$$SR = \frac{-b + \sqrt{b^2 + 4a}}{2a} \tag{42}$$

where $a = F_{11}\sigma_1^2 + F_{22}\sigma_2^2 + 2F_{12}\sigma_1\sigma_2 + F_{66}\sigma_{12}^2$, and $b = F_1\sigma_1 + F_2\sigma_2$. Setting a threshold SR^*, the margin of safety (MoS) can be defined as

$$MoS = SR - SR^* \tag{43}$$

SR^* can be chosen depending on the actual requirements, as long as it is larger than 1 to ensure the basic safety. MoS is an important index to evaluate the safety of the composite structure. The composite structure is considered to be safe if $MoS > 0$. It is interesting to study contributions of the input variables to MoS. In this application, it will take prohibitively long computational time to use MCS because the FEA model is very time-consuming to evaluate. As the proposed approach has been validated in previous examples, we directly use it to perform the sensitivity analysis in this application case.

It takes 504 calls to the FEA model to estimate the matrix $\boldsymbol{C}$. The eigenvalues are shown in Fig. 15. A total of 200 +26 = 226 calls to the FEA model are used to build the Kriging model in the one-dimensional active subspace, which is shown in Fig. 16. The GSA indices obtained by the proposed approach are given in Fig. 17. It clearly shows that

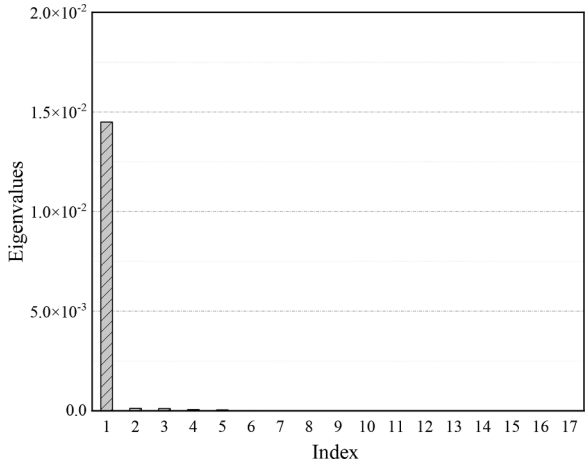

Fig. 15. The eigenvalues of the radome structure.

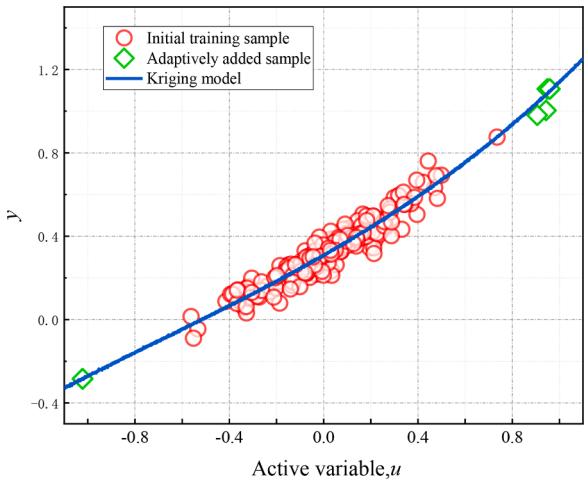

Fig. 16. The training samples and Kriging model in the active subspace of the radome structure.

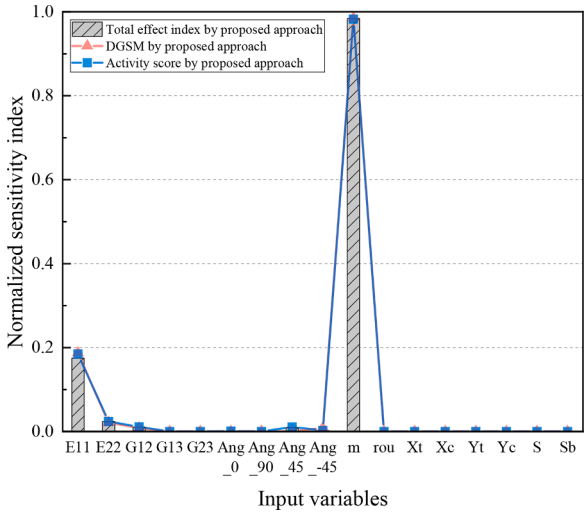

Fig. 17. GSA indices of the radome structure.

elastic modulus in the 11th direction E_{11} and thickness of single-layer plate m are the most significant variables to the safety of the composite radome.

6. Conclusion

In this work, we present computation of three different types of GSA indices carried out at different steps of the approach based on the theories of active subspace and Kriging. During the process of identifying the active subspace, the DGSM and activity score are obtained. After the identification of the active subspace, the Kriging model is built by an adaptive process to approximate the relationship between the active variables and the original model output. The Kriging model can be used to estimate the variance-based sensitivity indices such as Sobol' total effect indices. Tests have demonstrated the applicability and efficiency of the proposed approach. Besides being used for GSA, the underlying principle of the proposed approach can be further extended for other purposes such as reliability analysis, optimization.

The active subspace theory is a promising technique for model reduction especially for high-dimensional problems. It provides a novel perspective of probing into the input space by identifying the important directions, which motivates constriction of a surrogate model along these directions. This work shows the potential of the subspace theory in

the field of uncertainty analysis when dealing with high-dimensional problems. Issues such as efficient computation of the matrix **C** in the active subspace identification need further research.

CRediT authorship contribution statement

Changcong Zhou: Conceptualization, Methodology, Writing – review & editing, Formal analysis. **Zhuangke Shi:** Data curation, Formal analysis, Validation. **Sergei Kucherenko:** Methodology, Writing – review & editing, Formal analysis. **Haodong Zhao:** Software, Data curation.

Declaration of Competing Interest

The authors declare that they have no known competing financial interests or personal relationships that could have appeared to influence the work reported in this paper.

Acknowledgments

This work is supported by the National Natural Science Foundation of China (NSFC51975476), the Natural Science Basic Research Program of Shaanxi Province (2020JM-135), and the Aviation Science Foundation for the Aviation Key Laboratory of Science and Technology on Life-support Technology (20200029053001).

Appendix

The classical Kriging model is composed from a polynomial term for global trend prediction, and a Gaussian process term for local deviation regression [40]:

$$g_k(\boldsymbol{x}) = \boldsymbol{p}^{\mathrm{T}}(\boldsymbol{x})\boldsymbol{\beta} + z(\boldsymbol{x}) \tag{A.1}$$

where $\boldsymbol{p}(\boldsymbol{x})$ is the vector of polynomial basis functions, $\boldsymbol{\beta}$ is the vector of corresponding coefficients, and $z(\boldsymbol{x})$ is a Gaussian process of which the mean is zero. The covariance of $z(\boldsymbol{x})$ is given as

$$Cov\left(z(\boldsymbol{x}_i), z\left(\boldsymbol{x}_j\right)\right) = \sigma^2 R\left(\boldsymbol{x}_i, \boldsymbol{x}_j, \boldsymbol{\theta}\right) \tag{A.2}$$

where σ^2 is the variance of $z(\boldsymbol{x})$, and $R(\boldsymbol{x}_i, \boldsymbol{x}_j, \boldsymbol{\theta})$ is the correlation coefficient between $z(\boldsymbol{x}_i)$ and $z(\boldsymbol{x}_j)$ with parameters $\boldsymbol{\theta} = \{\theta_1, \theta_2, ..., \theta_n\}$. The Gaussian correlation function is used to control the smoothing of the Kriging model, which is defined as

$$R\left(\boldsymbol{x}_i, \boldsymbol{x}_j, \boldsymbol{\theta}\right) = \prod_{k=1}^{n} \exp\left(- \theta_k \left(x_i^{(k)} - x_j^{(k)}\right)^2\right) \tag{A.3}$$

where $x_i^{(k)}$ and $x_j^{(k)}$ are the kth coordinates of points $\boldsymbol{x}_i$ and $\boldsymbol{x}_j$. The parameters $\{\boldsymbol{\beta}, \sigma^2, \theta\}$ can be evaluated by a maximum likelihood estimation, represented as $\{\widehat{\beta}, \widehat{\sigma}^2, \widehat{\theta}\}$. With N training points $\{\mathbf{x}^{(l)}, \mathrm{g}(\mathbf{x}^{(l)})\}_{l=1,2,...,N}$, for a new point $\boldsymbol{x}$, the mean prediction $\widehat{g}_k(\boldsymbol{x})$ and mean square error (MSE) of the prediction can be estimated by the best linear unbiased estimation as follows:

$$\widehat{g}_k(\boldsymbol{x}) = \boldsymbol{p}^{\mathrm{T}}(\boldsymbol{x})\widehat{\beta} + \boldsymbol{r}^{\mathrm{T}}(\boldsymbol{x})\boldsymbol{R}^{-1}\left(\boldsymbol{g} - \boldsymbol{P}\widehat{\beta}\right) \tag{A.4}$$

$$MSE = \widehat{\sigma}^2\left[1 - \boldsymbol{r}^{\mathrm{T}}(\boldsymbol{x})\boldsymbol{R}^{-1}\boldsymbol{r}(\boldsymbol{x}) + \left(\boldsymbol{r}(\boldsymbol{x})\boldsymbol{R}^{-1}\boldsymbol{P} - \boldsymbol{p}(\boldsymbol{x})\right)^{\mathrm{T}}\left(\boldsymbol{P}^{\mathrm{T}}\boldsymbol{R}^{-1}\boldsymbol{P}\right)^{-1}\left(\boldsymbol{r}(\boldsymbol{x})\boldsymbol{R}^{-1}\boldsymbol{P} - \boldsymbol{p}(\boldsymbol{x})\right)\right] \tag{A.5}$$

Here $\boldsymbol{r}(\boldsymbol{x}) = [R(\boldsymbol{x}, \boldsymbol{x}_1), R(\boldsymbol{x}, \boldsymbol{x}_2), ...R(\boldsymbol{x}, \boldsymbol{x}_N)]^{\mathrm{T}}$ is the correlation vector between $\boldsymbol{x}$ and N training points, $\boldsymbol{R}$ is the correlation matrix, and $\boldsymbol{P} = [\boldsymbol{p}(\boldsymbol{x}^{(1)})^{\mathrm{T}}, \boldsymbol{p}(\boldsymbol{x}^{(2)})^{\mathrm{T}}, ..., \boldsymbol{p}(\boldsymbol{x}^{(N)})^{\mathrm{T}}]^{\mathrm{T}}$. The building of the Kriging model in this work is based on the MATLAB toolbox DACE [41].

References

[1] Saltelli A, Ratto M, Andres T, Francesca C. Global sensitivity analysis: the primer. Wiley; 2008.
[2] Borgonovo E, Hazen GB, Plischke E. A common rationale for global sensitivity measures and their estimation. Risk Anal 2016;36:1871–95.
[3] Wei PF, Lu ZZ, Song JW. Variable importance analysis, a comprehensive review. Reliab Eng Syst Saf 2015;142:399–432.
[4] Torii AJ, Novotny AA. A priori error estimates for local reliability-based sensitivity analysis with Monte Carlo simulation. Reliab Eng Syst Saf 2021;213:107749.
[5] Becker W. Metafunctions for benchmarking in sensitivity analysis. Reliab Eng Syst Saf 2020;204:107189.
[6] Ehre M, Papaioannou I, Straub D. A framework for global reliability sensitivity analysis in the presence of multi-uncertainty. Reliab Eng Syst Saf 2020;195:106726.
[7] Alexanderian A, Gremaud PA, Smith RC. Variance-based sensitivity analysis for time-dependent processes. Reliab Eng Syst Saf 2020;196:106722.
[8] Borgonovo E. A new uncertainty importance measure. Reliab Eng Syst Saf 2007;93:771–84.
[9] Kucherenko S, Song S, Wang L. Quantile based global sensitivity measures. Reliab Eng Syst Saf 2019;185:35–48.
[10] Sobol IM. Global sensitivity indices for nonlinear mathematical models and their Monte Carlo estimates. Math Comput Simul 2001;55:271–80.
[11] Saltelli A, Annoni P, Azzini I, Campolongo F, Ratto M, Tarantola S. Variance based sensitivity analysis of model output. Design and estimator for the total sensitivity index. Comput Phys Commun 2010;181:259–70.
[12] Lo Piano S, Ferretti F, Puy A, Albrecht D, Saltelli A. Variance-based sensitivity analysis: the quest for better estimators and designs between explorativity and economy. Reliab Eng Syst Saf 2021;206:107300.
[13] Kucherenko S, Rodriguez-Fernandez M, Pantelides C, Shah N. Monte Carlo evaluation of derivative-based global sensitivity measures. Reliab Eng Syst Saf 2009;94:1135–48.
[14] Morris MD. Factorial sampling plans for preliminary computational experiments. M Technometrics 1991;9:409–18.
[15] Sobol IM, Kucherenko S. Derivative based global sensitivity measures and their link with global sensitivity indices. Math Comput Simul 2009;79:3009–17.
[16] Lamboni M, Looss B, Popelin AL, Gamboa F. Derivative-based global sensitivity measures: general links with Sobol' indices and numerical tests. Math Comput Simul 2013;87:44–54.
[17] Zhou CC, Lu ZZ, Li LY, Feng J, Wang B. A new algorithm for variance based importance analysis of models with correlated inputs. Appl Math Model 2013;37:864–75.
[18] Zhou CC, Lu ZZ, Zhang F, Yue ZF. An adaptive reliability method combining relevance vector machine and importance sampling. Struct Multidiscip Optim 2015;52:945–57.
[19] Cheng K, Lu Z, Ling C, Zhou S. Surrogate-assisted global sensitivity analysis: an overview. Struct Multidiscip Optim 2020;61:1187–213.

[20] Liu H, Cai J, Ong YS. An adaptive sampling approach for Kriging metamodeling by maximizing expected prediction error. Comput Chem Eng 2017;106:171–82.
[21] Zhou YC, Lu ZZ, Jing JH, Hu YS. Surrogate modeling of high-dimensional problems via data-driven polynomial expansions and sparse partial least square. Comput. Methods Appl. Mech. Eng. 2020;364:112906.
[22] Constantine PG. Active subspaces: emerging ideas for dimension reduction in parameter studies. Philadelphia: SIAM; 2015.
[23] Li J, Cai J, Qu K. Surrogate-based aerodynamic shape optimization with the active subspace method. Struct Multidiscip Optim 2019;59:403–19.
[24] Cheng K, Lu ZZ. Hierarchical surrogate model with dimensionality reduction technique for high-dimensional uncertainty propagation. Int J Numer Methods Eng 2019;121:2068–85.
[25] Constantine PG, Diaz P. Global sensitivity metrics from active subspaces. Reliab Eng Syst Saf 2017;162:1–13.
[26] Homma T, Saltelli A. Importance measures in global sensitivity analysis of model output. Reliab Eng Syst Saf 1996;52:1–17.
[27] Campolongo F, Cariboni J, Saltelli A. An effective screening design for sensitivity analysis of large models. Environ Model Softw 2007;22:1509–18.
[28] Kucherenko S, Looss B. Derivative-based global sensitivity measures. Handbook of uncertainty quantification. Springer; 2017. p. 1241–63.
[29] Constantine PG, Dow E, Wang Q. Active subspace methods in theory and practice: applications to kriging surfaces. SIAM J. Sci. Comput. 2014;36. A1500–A1524.
[30] Liu H, Ong YS, Cai J. A survey of adaptive sampling for global metamodeling in support of simulation-based complex engineering design. Struct. Multidisc. Optim. 2018;57:393–416. 2018.
[31] Sobol IM, Asotsky D, Kreinin A, Kucherenko S. Construction and comparison of high-dimensional Sobol' generators, 56. Wilmott; 2011. p. 64–79. J.
[32] Kucherenko S., Albrecht D., Saltelli A., Exploring multi-dimensional spaces: a comparison of Latin Hypercube and quasi Monte Carlo sampling techniques, 2015, arXiv:1505.02350.
[33] Molkenthin C, Scherbaum F, Griewank A, Leovey H, Kucherenko S, Cotton F. Derivative-based global sensitivity analysis: upper bounding of sensitivities in seismic-hazard assessment using automatic differentiation. B Seismol Soc Am 2017;107:984–1004.
[34] Peng Z.Z., Uncertainty analysis and experimental calibration methods of thermal structure model of composite materials, Ph.D. thesis, Harbin Institute of Technology, Harbin, 2018. (in Chinese).
[35] Constantine P.G., Gleich D., Computing active subspaces with Monte Carlo, 2014, arXiv: 1408.0545.
[36] Russi T.M., Uncertainty quantification with experimental data and complex system models, Ph.D. thesis, University of California, Berkeley, 2010.
[37] Jansen MJW. Analysis of variance designs for model output. Comput Phys Commun 1999;117:35–43.
[38] Li LY, Lu ZZ, Feng J, Feng BT. Moment-independent importance measure of basic variable and its state dependent parameter solution. Struct Saf 2012;38:40–7.
[39] Kaw AK. Mechanics of composite materials. CRC Press; 2005.
[40] Rasmussen CE. Gaussian processes for machine learning. The MIT Press; 2006.
[41] S.N. Lophaven, H.B. Nielsen, J. Sondergaard, DACE-A MATLAB Kriging toolbox, version 2.0. Technical University of Denmark, Lyngby, 2002.